Received: 7 February 2019 | Revised: 1 July 2019 | Accepted: 2 July 2019

DOI: 10.1111/jzs.12330

ORIGINAL ARTICLE

JOURNAL OF ZOOLOGICAL SYSTEMATICS AND EVOLUTIONARY RESEARCH

WILEY

Phylogeography and population history of the least weasel (*Mustela nivalis*) in the Palearctic based on multilocus analysis

Takuma Sato[1] | Alexei V. Abramov[2] | Evgeniy G. Raichev[3] | Pavel A. Kosintsev[4,5] | Risto Väinölä[6] | Takahiro Murakami[7] | Yayoi Kaneko[8] | Ryuichi Masuda[1,9]

[1]Department of Natural History Sciences, Graduate School of Science, Hokkaido University, Sapporo, Japan

[2]Zoological Institute, Russian Academy of Sciences, St. Petersburg, Russia

[3]Agricultural Faculty, Trakia University, Stara Zagora, Bulgaria

[4]Institute of Plant and Animal Ecology, Ural Branch, Russian Academy of Sciences, Ekaterinburg, Russia

[5]Ural Federal University, Ekaterinburg, Russia

[6]Finnish Museum of Natural History, University of Helsinki, Helsinki, Finland

[7]Shiretoko Museum, Shari, Japan

[8]Faculty of Agriculture, Tokyo University of Agriculture and Technology, Fuchu, Japan

[9]Department of Biological Sciences, Faculty of Science, Hokkaido University, Sapporo, Japan

Correspondence
Ryuichi Masuda, Department of Biological Sciences, Faculty of Science, Hokkaido University, Sapporo 060-0810, Japan.
Email: masudary@sci.hokudai.ac.jp

Funding information
Russian Foundation for Basic Research, Grant/Award Number: AAAA-A17-117022810195-3; Japan Arctic Research Network Center; Japan Society of the Promotion of Science (JSPS)

Abstract

The least weasel (*Mustela nivalis*) is one of the most widely distributed carnivorans. While previous studies have identified distinct western and eastern mitochondrial DNA (mtDNA) lineages of the species in the western Palearctic, their broader distributions across the Palearctic have remained unknown. To address the broad-scale phylogeographical structure, we expanded the sampling to populations in Eastern Europe, the Urals, the Russian Far East, and Japan, and analyzed the mtDNA control region and cytochrome *b*, the final intron of the zinc finger protein on Y chromosome (*ZFY*), and the autosomal agouti signaling protein gene (*ASIP*). The mtDNA data analysis exposed the previous western lineage (Clade I) but poorly supported assemblage extending across Palearctic, whereas the previous eastern lineage (Clade II) was reconfirmed and limited in the south western part of the Palearctic. The *ZFY* phylogeny showed a distinctive split that corresponding to the mtDNA lineage split, although less phylogeographical structure was seen in the *ASIP* variation. Our data concur with the previous inference of the Black Sea–Caspian Sea area having an ancestral character. The Urals region harbored high mitochondrial diversity, with an estimated coalescent time of around 100,000 years, suggesting this could have been a cryptic refugium. Based on the coalescent-based demographic reconstructions, the expansion of Clade I across the Palearctic was remarkably rapid, while Clade II was relatively stable for a longer time. It seems that Clade II has maintained a constant population size in the temperate region, and the expansive Clade I represents adaptation to the cold regions.

KEYWORDS

ASIP, least weasel, mitochondrial DNA, *Mustela nivalis*, *ZFY*

Contributing authors: Takuma Sato (takuma.s.310@gmail.com); Alexei V. Abramov (a.abramov@mail.ru); Evgeniy G. Raichev (eraichev@uni-sz.bg); Pavel A. Kosintsev (kpa@ipae.uran.ru); Risto Väinölä (risto.vainola@helsinki.fi); Takahiro Murakami (murataka@cf7.so-net.ne.jp); Yayoi Kaneko (ykaneko7946@gmail.com)

1 | INTRODUCTION

Some species have narrow distributions within limited geographic regions, while others are distributed broadly across the globe. A basic concern of biogeographical science is to understand how species have evolved and acquired their worldwide distributions. Phylogeography explores the evolutionary and dispersal histories of widespread species using the genealogical information embedded in their DNA (Garrick et al., 2015). Many studies of phylogeography have tried to reconstruct the migration histories of mammalian species in the Palearctic and to identify their glacial refugia, which have frequently been located in the Balkan and Iberian peninsulas, in the Caucasus and the Russian Far East (Frantz et al., 2014; Hewitt, 1999; Hope et al., 2010; Korsten et al., 2009). The location of these refugia evidently reflects the species' environmental tolerances (Schmitt & Varga, 2012). Moreover, Řičánková, Robovský, Riegert, and Zrzavý (2015) pointed out that Central Asia was important as a glacial refugium for the megafauna and that the "mammoth fauna" (these were the cold tolerant fauna, which developed and reached their peak during the late Pleistocene, see Vereshchagin & Baryshnikov, 1992) remained there with highest frequency in Palearctic.

The least weasel (*Mustela nivalis* Linnaeus, 1766) is one of the most widespread carnivore taxa in the Northern Hemisphere with a range covering most of the Palearctic: Europe, North Africa, Northern Asia including the Japanese islands, and North America. Considering this fossil records, the least weasel is included in the "mammoth fauna" (Sheffield & King, 1994; Youngman, 1993, and references therein). This species is considered a mesopredator, and their diet consists mainly of rodents, lagomorphs with some insects (King & Powell, 2007). The least weasel has significant variation in body and skull sizes and proportions throughout its huge distribution range (Abramov & Baryshnikov, 2000). Along with an overall high variation of cranial characters, there is a tendency toward an increase in body size and relative tail length from the north to south and to some extent from the east to west (Abramov & Baryshnikov, 2000). Abramov and Baryshnikov also suggested the least weasel has unique geographical variations such as the distribution of the two pelage colorations (*nivalis* and *vulgaris*): The *nivalis* type is distributed in northern Palearctic and the *vulgaris* type in the Mediterranean region, and the ancestral cranial type, in turn, is distributed in Northern Africa, Spain, Caucasus, Middle East, and Central Asia. It is also remarkable that the body sizes of the least weasels do not follow the Bergmann rule (Bergmann, 1847). King and Powell (2007) suggested that this phenomenon is affected by the unique evolutionary process of the least weasels, which have decreased their body sizes so that they can prevent the heat loss and forage the small rodents in the cold environment. In fact, Marciszak and Socha (2014) reported a correlation between the temperature and the cranial size using the fossil materials from Polish caves: The size decreases during colder periods and increases in warmer intervals. In addition, Zub, Szafrańska, Konarzewski, and Speakman (2011) suggested the winter survival rate is higher for smaller than for larger least weasels. It is plausible that several weasel characters including the ecological status, comprehensive distribution, and great geographical variation have resulted from adaptation to the various environments, and it is interesting to further understand the evolutionary history of the least weasel.

The chromosome number of the least weasel in Siberia and in Hokkaido, Japan, is $2n = 42$, whereas on the Honshu Island it is $2n = 38$ (Mandahl & Fredga, 1980; Obara, 1991). Distinct mitochondrial DNA (mtDNA) control region (*CR*) sequences were observed in least weasels from Hokkaido and Honshu islands, as reported by Kurose, Masuda, and Yoshida (1999). In a phylogeographic analysis of the mtDNA *CR* across Siberia, the Caucasus, Central Asia, and North America, the lineages around the Caucasus were the most variable probably due to the introgression or maintenance of polymorphic status of their ancestral population (Kurose, Abramov, & Masuda, 2005). Meanwhile, Lebarbenchon, Poitevin, Arnal, and Montgelard (2010) detected a subdivision of the Western Palearctic least weasel mitochondrial diversity into Western (Clade I) and Eastern (Clade II) lineages using the mtDNA *CR* and cytochrome *b* (*Cytb*) sequences. Using only *Cytb* data, Mcdevitt et al. (2012) identified a presence of a suture zone between the lineages in Poland and suggested that the Carpathians were one of the refugia for the least weasel and confirmed the existence of the two main lineages, similar to the western Palearctic region reported by Lebarbenchon et al. (2010). Rodrigues et al. (2016) revealed the taxonomic status of the Egyptian least weasel that shared a haplotype with weasels in Turkey and Mediterranean islands. Additionally, the least weasel could have been imported to some Mediterranean islands artificially, and the gene flow could have affected the genetic structure (Lebarbenchon et al., 2010; Rodrigues et al., 2017). However, the original dispersal and migration history of the least weasels still remains unclear in Palearctic.

To further understand the molecular phylogenetic and biogeographical relationships among least weasels, we have analyzed mtDNA *CR* and *Cytb*, as maternally inherited genes, from a range of new localities across the Palearctic region. In addition, we also sequenced and analyzed the final intron of the zinc finger protein locus on the Y chromosome (*ZFY*) as a paternally inherited gene and the agouti signaling protein locus (*ASIP*) as a biparentally inherited gene. Combining our data with the previous results, we discuss the phylogeography and migration history of the least weasel in Palearctic.

2 | MATERIALS AND METHODS

2.1 | Specimens

Tissue samples were obtained from collaborative laboratories and museums in Bulgaria, Russia, Finland, and Japan (76 samples consisting of 65 ethanol-preserved muscle tissues and 11 dried skins; Table 1 and Figure 1). Of these, 31 were also used in the previous mtDNA *CR* studies of Kurose et al. (1999), Kurose et al. (2005). In

TABLE 1 Geographic origins and accession numbers of samples examined in this study

Voucher No.	Geographic origins	Accession Nos.			
		CR	*Cytb*	*ZFY*	*ASIP*
Mn4	Japan, Hokkaido, Shari-cho	LC314620	LC324904	LC325040	LC324973
Mn5	Japan, Hokkaido, Shari-cho	LC314621	LC324905	–	LC324974
Mn6	Japan, Hokkaido, Shari-cho	LC314624	LC324906	–	LC324975
Mn7	Japan, Hokkaido, Shari-cho	LC314622	LC324907	–	LC324976
NEM01	Japan, Hokkaido, Nemuro	LC314625	LC324908	–	LC324977
OBH01	Japan, Hokkaido, Obihiro	LC314623	LC324909	–	LC324978
S12	Japan, Hokkaido, Shari-cho	AB006720[a]	LC324910	LC325041	LC324979
S13	Japan, Hokkaido, Shari-cho	AB006721[a]	–	–	LC324980
S14	Japan, Hokkaido, Shari-cho	Same as S13[a]	LC324911	LC325042	LC324981
YOT1	Japan, Hokkaido, Mt. Yōtei	AB006719[a]	LC324912	–	LC324982
OB1	Japan, Hokkaido, Makubetsu-cho	AB006718[a]	LC324913	LC325043	LC324983
OB2	Japan, Hokkaido, Shihoro-cho	Same as S13[a]	LC324914	–	LC324984
HIT1	Japan, Hokkaido, Sapporo	AB006722[a]	LC324915	–	LC324985
HIT2	Japan, Hokkaido, Sapporo	AB006723[a]	LC324916	LC325044	LC324986
N26	Japan, Hokkaido, Unknown	AB006724[a]	LC324917	LC325045	LC324987
N27	Japan, Hokkaido, Sapporo	AB006725[a]	LC324918	LC325046	LC324988
N28	Japan, Hokkaido, Sapporo	Same as N27[a]	LC324919	–	LC324989
N29	Japan, Hokkaido, Sapporo	Same as N27[a]	LC324920	–	LC324990
N30	Japan, Hokkaido, Sapporo	AB006726[a]	LC324921	–	LC324991
N31	Japan, Hokkaido, Sapporo	Same as YOT1[a]	LC324922	LC325047	LC324992
N32	Japan, Hokkaido, Shibecha-cho	AB006727[a]	LC324923	LC325048	LC324993
N33	Japan, Hokkaido, Sapporo	Same as N30[a]	LC324924	LC325049	LC324994
N34	Japan, Hokkaido, Sapporo	Same as HIT1[a]	LC324925	–	LC324995
N35	Japan, Hokkaido, Shibecha-cho	Same as N32[a]	LC324926	–	LC324996
N37	Japan, Hokkaido, Sapporo	Same as HIT1[a]	LC324927	–	LC324997
AKI1	Japan, Akita, Kazuno-shi	AB006728[a]	LC324928	LC325050	LC324998
IWA1	Japan, Iwate, Kunohe-gun	Same as AKI1[a]	LC324929	AB491594[c]	LC324999
IWA2	Japan, Iwate, Iwaizumi-cho	Same as AKI1[a]	LC324930	LC325051	LC325000
151646	Russia, Staroutkinsk	LC314601	LC324931	–	LC325001
278252	Russia, Karpinsk	LC314602	LC324932	–	LC325002
79252	Russia, Priuralsky District	LC314603	LC324933	–	–
79253	Russia, Priuralsky District	LC314604	–	–	–
79254	Russia, Priuralsky District	LC314605	–	–	–
79255	Russia, Priuralsky District	LC314606	LC324934	–	LC325003
79271	Russia, oz. Yarato 2-e	LC314607	LC324935	LC325052	–
79272	Russia, oz. Yarato 2-e	LC314608	–	–	–
79273	Russia, oz. Yarato 2-e	LC314609	–	–	–
79274	Russia, Yamalsky District	LC314610	–	–	–
79304	Russia, Yamalsky District	LC314611	LC324936	–	LC325004
79307	Russia, Priuralsky District	LC314612	LC324937	–	LC325005
RLEN3	Russia, Leningrad Province	Same as RALTI[b]	LC324938	LC325053	LC325006
RIND1	Russia, Indigirka	AB049772[b]	LC324939	–	LC325007
ROMS1	Russia, Omsk, West Siberia	LC314613	–	–	–
BUSG1	Bulgaria, Sredna Gora	LC314614	LC324940	LC325054	LC325008

(Continues)

TABLE 1 (Continued)

Voucher No.	Geographic origins	Accession Nos.			
		CR	*Cytb*	*ZFY*	*ASIP*
BUV1	Bulgaria, Varna	LC314615	LC324941	LC325055	LC325009
BUV2	Bulgaria, Varna	LC314616	LC324942	LC325056	LC325010
BUV3	Bulgaria, Varna	LC314617	LC324943	LC325057	LC325011
BUV4	Bulgaria, Varna	LC314618	LC324944	LC325058	LC325012
BUV5	Bulgaria, Varna	LC314619	LC324945	LC325059	LC325013
RTUR2	Turkmenistan, Murgab	Same as RCAU1[b]	LC324946	–	LC325014
RKAR2	Turkmenistan, South East Karakum	AB049774[b]	LC324947	–	LC325015
RASK1	Ukraine, Askania, Nova	AB049765[b]	LC324948	–	LC325016
RASK2	Ukraine, Askania, Nova	AB049768[b]	LC324949	–	LC325017
RUMA1	Ukraine, Kiev Province	Same as RALTI[b]	LC324950	–	LC325018
RCAC1	Georgia, Tbilisi	AB049770[b]	LC324951	–	–
RCAU2	Georgia, Lagodekhi	AB049771[b]	LC324952	–	LC325019
KS.KN 39356	Finland, Porvoon mlk	LC314626	LC324953	LC325060	LC325020
KS.KN 39357	Finland, Joutsa	LC314627	LC324954	LC325061	LC325021
KS.KN 34388	Finland, Siuntio	LC314628	LC324955	–	LC325022
KS.KN 34462	Finland, Helsinki, Vuosaari	LC314629	LC324956	–	LC325023
KS.KN 34463	Finland, Inkoo	LC314630	LC324957	–	LC325024
KS.KN 39310	Finland, Heinolan mlk	LC314631	LC324958	–	LC325025
KS.KN 34644	Finland, Vantaa, Korso	LC314632	LC324959	–	LC325026
KS.KN 38719	Finland, Siuntio	LC314633	LC324960	–	LC325027
KS.KN 34740	Finland, Vihti, Selki	LC314634	LC324961	–	LC325028
KS.KN 33901	Finland, Vantaa, Riipilä	LC314635	LC324962	–	LC325029
KS.KN 47736	Finland, Finström	LC314636	LC324963	LC325062	LC325030
KS.KN 47078	Finland, Dragsfjärd	LC314637	LC324964	LC325063	LC325031
KS.KN 47020	Finland, Keuruu, Haapamäki	LC314638	LC324965	LC325064	LC325032
KS.KN 47872	Finland, Espoo	LC314639	LC324966	LC325065	LC325033
KS.KN 47874	Finland, Tampere	LC314640	LC324967	LC325066	LC325034
KS.KN 47882	Finland, Asikkala	LC314641	LC324968	LC325067	LC325035
KS.KN 47906	Finland, Pernaja	LC314642	LC324969	–	LC325036
KS.KN 47907	Finland, Porvoo	LC314643	LC324970	LC325068	LC325037
KS.KN 48312	Finland, Heinävesi	LC314644	LC324971	–	LC325038
KS.KN 48372	Finland, Kuhmo	LC314645	LC324972	–	LC325039

[a]Kurose et al. (1999).
[b]Kurose et al. (2005).
[c]Yamada and Masuda (2010).

addition, we employed published data from public databases, as specified in Tables 1 and S1.

2.2 | DNA extraction, amplification, and sequencing

Total DNA was extracted from the samples using the DNeasy Tissue & Blood Kit (QIAGEN) or QIAamp DNA Investigator Kit (QIAGEN), following the manufacturer's protocols, including extraction blanks for the negative control. All experiments were done with filter tips and disposal tubes for preventing the contamination in the present study.

Two fragments of the mtDNA, *CR* (around 550 base-pairs, bp) and *Cytb* (1,140 bp), and one from the Y-chromosomal *ZFY* (687 bp) and one from autosomal *ASIP* gene (480 bp; intron and exon), were amplified by PCR with the primers shown in Table S2. For DNA degraded samples, we amplified small fragments (165–705 bp) overlapping each other. In the samples of dried skins, relatively shorter DNA fragments were amplified. Furthermore, we duplicated the experiments for the data confirmation on the degraded samples.

PCR was carried out in a volume of 10 μl including 2.0 μl of 5× Prime STAR GXL DNA Buffer (Takara), 0.8 μl of dNTP mixture

(2.5 mM each dNTP; Takara), 0.2 μl of Prime STAR GXL DNA Polymerase (1.25 U/μl, Takara), 0.4 μl for each of forward and reverse primers (10 pmol/μl), 0.4 of bovine serum albumin (0.4 μg/μl, Roche), and 1.0–2.0 μl of the DNA extract, and the volume was adjusted to a total of 10 μl with distilled water. The amplification was performed with 30–45 cycles of 98°C for 10 s, 54–61.4°C for 15 s, and 68°C for 1min using the Thermal Cycler TP400 (Takara). To check the amplicon, 3μl of the PCR product was electrophoresed on a 2% agarose gel, stained with ethidium bromide, and observed under an ultraviolet illumination. Then, the PCR products were purified with the QIAquick PCR Purification Kit (QIAGEN). In addition, we confirmed no PCR amplification in the negative controls.

The DNA cycle sequencing was performed with the BigDye v3.1 or 1.1 Cycle Sequencing Kit (Applied Biosystems, ABI), using the PCR primers shown in Table S2. Sequencing reaction was performed in a volume of 10 μl containing 1.75 μl of 5× BigDye Sequencing Buffer (ABI), 0.5 μl of Ready Reaction Premix (ABI), 0.5 μl for each of the primers, and 2.0 μl of DNA template, and the volume was adjusted to 10 μl with distilled water. Cycle sequencing was performed with a preheating at 96°C for 1 min and 25 cycles of 96°C for 10 s, 50°C or 55°C for 5 s, and 60°C for 4 min. The cycle PCR products were precipitated with ethanol, and dissolved in 10 μl of formamide, and applied to an ABI 3,730 DNA Analyzer for sequencing. The sequence alignment for all loci was performed using MUSCLE in MEGA6 (Tamura, Stecher, Peterson, Filipski, & Kumar, 2013).

2.3 | Phylogenetic trees and networks

The nucleotide substitution models for analyses of all loci were selected using the Bayesian information criterion (BIC) with PartitionFinder v1.1.1 (Lanfear, Calcott, Ho, & Guindon, 2012). The selected models were used to reconstruct phylogenetic trees (gene genealogies) with two approaches and programs: MrBayes v3.2.6 (Ronquist et al., 2012) for analyses under Bayesian inference (BI) and Garli v2.01 (Bazinet, Zwickl, & Cummings, 2014) for Heuristic maximum-likelihood analyses (ML). For analysis of the concatenated *CR* and *Cytb* sequence segments, separate substitution models were estimated for the *CR* segment and for each of three codon positions in the *Cytb* (1,2,3): These were K81uf + I + G, K80 + G, HKY, and TrN + G, but in the phylogenetic analysis HKY and GTR models were used instead of K81uf and TrN models, respectively, because these models were not implemented in MrBayes (Hasegawa, Kishino, & Yano, 1985; Kimura, 1980, 1981; Lanave, Preparata, Saccone, & Serio, 1984; Tamura & Nei, 1993). The list of the other nucleotide substitution models is shown in Table S3.

For the BI trees, Markov chain Monte Carlo (MCMC) analyses were run for 5×10^6 to 1×10^7 generations with trees sampled every 1,000 generations, and the first 25% of the trees were discarded as burn-in. The convergence of MCMC analyses was confirmed by indicating the average standard deviation of split frequencies was below <0.01, and the parameter values sampled from MCMC runs were checked in Tracer ver. 1.6 (http://tree.bio.ed.ac.uk/software/tracer/). The Bayesian posterior probabilities (PP) were also obtained from MrBayes. In the reconstruction of the ML trees, the effort to search for the best tree was repeated 20 times independently and terminated at 20,000 generations with Garli. The maximum-likelihood bootstrap percentages (BP) were obtained from 1,000 pseudoreplicates with Garli to assess the confidence values of tree nodes.

Two confidence values (PP and BP) for the reconstructed nodes were mapped on the trees using SumTrees 3.3.1 of the DendroPy package (Sukumaran & Holder, 2010). Nodes of the trees were regarded as well supported when their PP was ≥0.95 and BP was ≥70%. Haplotypes from other three closely related species (*Mustela nudipes* Desmarest, 1822: AB601587 for *CR*, AB285332 for *Cytb*; *M. kathiah* Hodgson, 1835: AB601575, AB285331; *M. erminea* L., 1758: AB006730, AB026101) were used as outgroups in the mtDNA tree. The *M. erminea* sequences of *ZFY* and *ASIP* (AB491595 and JX130732, respectively) were used as the references for these genes. The SINEs (short interspersed nuclear elements) region of the *M. erminea's ZFY* sequence was excluded in the analysis. These phylogenetic trees were visualized and edited with FigTree v1.4.2 (http://tree.bio.ed.ac.uk/software/figtree/).

Median-joining networks of the concatenated mtDNA *CR* and *Cytb*, of *ZFY*, and of *ASIP* separately were reconstructed with POPART 1.7 (Leigh & Bryant, 2015). The program PHASE implemented in DnaSP v5 (Librado & Rozas, 2009) was used to estimate the haplotypes of *ASIP*. In all network analysis, the gap sites were treated as missing.

2.4 | Divergence time and demographic history

Population divergence times were estimated from the concatenated mtDNA two-locus data set using BEAST v2.4.8 (Bouckaert et al., 2014) package, with the outgroups mentioned above. Three calibration points were set on the basis of the divergence times among outgroup species and least weasels. Following Sato et al. (2012) and Kinoshita et al. (2015), a normal distribution with a mean of following time and *SD* was adopted to this analysis: 5.985 ± 0.315 million years ago (mya) between *M. nudipes* and the others, 5.365 ± 0.195 mya between *M. kathiah* and the others except *M. nudipes*, and 3.685 ± 0.285 mya between *M. erminea* and *M. nivalis*. In addition, the published estimate of least weasel mtDNA *Cytb* substitution rate of 2.1% Myr^{-1} from Dawson, Hope, Talbot, and Cook (2014) and the strict clock model were also used. The tree prior was set as the coalescent constant population model. The HKY + I + G substitution model was used for all loci, which was the best model for our data without partitions using BIC produced by PartitionFinder. The evolutionary rates of other loci were estimated based on these configurations. The MCMC analyses were run 1×10^8 generations with trees sampled every 1,000 generations, and the first 10% of the trees were discarded as burn-in. The effective sample sizes were confirmed by Tracer, with the requirements of convergence of MCMC chains and values for all parameters exceeding 200. The maximum clade credibility tree was selected using TreeAnnotator and visualized with FigTree.

FIGURE 1 Sampling locations. The samples examined in the present study are shown as diamonds, and the detailed localities are shown in Table 1. According to the previous studies (Hosoda et al., 2000, 2011; Kurose, Abramov, & Masuda, 2000; Kurose et al., 2005, 1999; Lebarbenchon et al., 2010; Lebarbenchon, Poitevin, & Montgelard, 2006; Mcdevitt et al., 2012; Rodrigues et al., 2016), the reference localities are shown as circles and the detailed localities were indicated in Table S1. If the samples did not have detailed sampling localities in the previous studies, their plots were located at the metropolis of each country or prefecture. The gray color means the distribution range of least weasel in the Palearctic, modified from McDonald et al. (2016)

Demographic changes (effective population size history) were simulated by the Extended Bayesian Skyline Plot (EBSP) approached in BEAST. The HKY + I + G model and the substitution rate of 2.1% Myr^{-1} for the mtDNA *Cytb* of the least weasel were applied to each of the two identified main mitochondrial clades separately (Clades I and II; 106 and 56 individuals, respectively). The MCMC analyzes were run 1×10^8 generations with trees sampled every 1,000 generations, and the first 10% of the trees were discarded as burn-in. The effective sample sizes and the convergence of MCMC chains were confirmed by Tracer.

2.5 | Genetic structure

Genetic diversity and demographic history were estimated from each data set separately (i.e., concatenated mtDNA *CR* and *Cytb*, *ZFY*, and *ASIP*) with Arlequin ver. 3.5.1.3 (Excoffier & Lischer, 2010), calculating the haplotype diversity, the nucleotide diversity, the neutrality tests of Tajima's *D* (Tajima, 1989), and Fu's F_s (Fu, 1997).

Population structure was also assessed with SAMOVA (spatial analyses of molecular variance; Dupanloup, Schneider, & Excoffier, 2002) implemented in SPADS 1.0 (Dellicour & Mardulyn, 2014), using all 168 concatenated mtDNA *CR* and *Cytb* sequences. Specimens were grouped as populations by country, except for Japan where Hokkaido and Honshu were treated as different populations because there is a chromosomal difference between them. The number of a priori groups (*K*) was varied between 2 and 10, with 10,000 iterations and 10 repetitions. Following Magri et al. (2006), the preferred *K* was selected by choosing the highest F_{CT}, and then, configurations with single-population groups were excluded. In addition, the pairwise differences among populations were estimated using the fixation index Φ_{st} (Excoffier, Smouse, & Quattro, 1992).

3 | RESULTS

3.1 | DNA sequencing

A total of 210 novel sequences (45 for *CR*, 69 for *Cytb*, 29 for *ZFY* and 67 for *ASIP*) were obtained in the present study and deposited to the DDBJ database with accession numbers: *CR*, LC314601-LC314645; *Cytb*, LC324904-LC324972; *ZFY*, LC325040-LC325068; and *ASIP*, LC324973-LC325039 (Table 1). In the alignments, the novel sequences were compared with the previously reported data (Tables 1 and S1), and then, overlapped regions were used to classify the haplotypes. All haplotype numbers were shown in Tables 2 and S1.

3.2 | Diversity and genealogy of mtdna

In all, 92 distinct haplotypes were identified from the 215 sequences of the mtDNA *CR*. The length of *CR* was 514 bp including insert–deletion sites. The BI tree of *CR* was multifurcate and unstructured with no clear clusters except for the Hokkaido population (Cluster Ie; Figure S1 and Alignment S1). Likewise, 116 haplotypes of *Cytb* were detected from 221 sequences of 1,117 bp. The BI tree of *Cytb* was also poorly resolved, but some populations including the Hokkaido population and some European populations made up regional clusters (Figure S2 and Alignment S2).

TABLE 2 Haplotype numbers of samples examined in this study

	Haplotype Nos.									
Voucher No.	*CR*	*Cytb*	*CR* and *Cytb*	*ZFY*	*ASIP*-1	*ASIP*-2	*mtDNA* and *ZFY*	*mtDNA* and *ASIP*	*ZFY* and *ASIP*	ALL
Mn4	A16	B53	C63	D1	E9	E9	F17	G40	H2	I19
Mn5	A16	B23	C22	–	E9	E9	–	G2	–	–
Mn6	A33	B23	C53	–	E9	E9	–	G31	–	–
Mn7	A16	B23	C22	–	E9	E9	–	G2	–	–
NEM01	A33	B23	C53	–	E9	E9	–	G31	–	–
OBH01	A30	B23	C38	–	E9	E9	–	G12	–	–
S12	A17	B24	C23	D1	E9	E9	F2	G3	H2	I2
S13	A16	–	–	–	E9	E9	–	–	–	–
S14	A16	B23	C22	D1	E9	E12	F1	G2	H1	I1
YOT1	A2	B2	C2	–	E9	E9	–	G1	–	–
OB1	A31	B23	C40	D1	E9	E9	F4	G14	H2	I4
OB2	A16	B38	C39	–	E9	E9	–	G13	H11	–
HIT1	A34	B23	C54	–	E1	E9	–	G33	H11	–
HIT2	A30	B23	C38	D1	E1	E9	F19	G12	H4	I20
N26	A37	B23	C58	D1	E6	E6	F14	G39	H8	I18
N27	A36	B23	C57	D1	E6	E6	F16	G38	H8	I17
N28	A36	B23	C57	–	E6	E6	–	G38	H11	–
N29	A36	B23	C57	–	E6	E6	–	G38	H11	–
N30	A35	B23	C55	–	E6	E6	–	G37	H11	–
N31	A2	B48	C56	D1	E9	E6	F15	G36	H3	I16
N32	A33	B23	C53	D1	E9	E9	F13	G31	H2	I15
N33	A35	B23	C55	D1	E9	E9	F12	G35	H2	I14
N34	A34	B23	C54	–	E6	E6	–	G34	H12	–
N35	A33	B23	C53	–	E9	E9	–	G31	H12	–
N37	A34	B23	C54	–	E9	E9	–	G32	H12	–
AKI1	A45	B59	C66	D1	E5	E5	F18	G41	H12	I27
IWA1	A45	B59	C66	D1	E5	E5	F18	G41	H12	I27
IWA2	A45	B59	C66	D1	E5	E5	F18	G41	H12	I27
151646	A27	B88	C118	–	E1	E2	–	G52	–	–
278252	A43	B87	C115	–	E2	E2	–	G51	–	–
79252	A77	B86	C109	–	–	–	–	–	–	–
79253	A79	–	–	–	–	–	–	–	–	–
79254	A80	–	–	–	–	–	–	–	–	–
79255	A76	B85	C108	–	E3	E3	–	G50	–	–
79271	A75	B84	C107	D1	–	–	F26	–	–	–
79272	A81	–	–	–	–	–	–	–	–	–
79273	A82	–	–	–	–	–	–	–	–	–
79274	A83	–	–	–	–	–	–	–	–	–
79304	A74	B83	C106	–	E2	E2	–	G49	–	–
79307	A73	B82	C105	–	E4	E4	–	G48	–	–
RLEN3	A18	B27	C27	D1	E2	E2	F3	G6	H5	I3
RIND1	A21	B30	C29	–	E1	E1	–	G8	–	–
ROMS1	A74	–	–	–	–	–	–	–	–	–

(Continues)

TABLE 2 (Continued)

	Haplotype Nos.									
Voucher No.	*CR*	*Cytb*	*CR* and *Cytb*	*ZFY*	*ASIP*-1	*ASIP*-2	*mtDNA* and *ZFY*	*mtDNA* and *ASIP*	*ZFY* and *ASIP*	ALL
BUSG1	A15	B79	C102	D2	E2	E2	F25	G47	H11	I26
BUV1	A11	B78	C101	D2	E2	E2	F24	G46	H11	I25
BUV2	A70	B77	C100	D2	E2	E2	F23	G45	H11	I24
BUV3	A64	B76	C99	D2	E2	E2	F22	G44	H11	I23
BUV4	A69	B75	C98	D2	E2	E2	F21	G43	H11	I22
BUV5	A64	B74	C97	D2	E1	E2	F20	G42	H10	I21
RTUR2	A19	B26	C25	–	E10	E2	–	G5	–	–
RKAR2	A20	B29	C28	–	E2	E2	–	G7	–	–
RASK1	A25	B34	C33	–	E1	E2	–	G11	–	–
RASK2	A24	B33	C32	–	E1	E6	–	G10	–	–
RUMA1	A18	B25	C24	–	E2	E11	–	G4	–	–
RCAC1	A23	B32	C31	–	–	–	–	–	–	–
RCAU2	A22	B31	C30	–	E1	E1	–	G9	–	–
KS.KN 39356	A73	B47	C52	D1	E1	E1	F11	G30	H9	I13
KS.KN 39357	A27	B28	C44	D1	E2	E7	F5	G21	H6	I5
KS.KN 34388	A73	B41	C45	–	E2	E2	–	G22	–	–
KS.KN 34462	A27	B28	C44	–	E2	E2	–	G20	–	–
KS.KN 34463	A27	B28	C44	–	E1	E1	–	G18	–	–
KS.KN 39310	A27	B28	C44	–	E1	E8	–	G17	–	–
KS.KN 34644	A59	B28	C43	–	E2	E2	–	G16	–	–
KS.KN 38719	A59	B40	C42	–	E2	E2	–	G15	–	–
KS.KN 34740	A59	B40	C42	–	E2	E2	–	G15	–	–
KS.KN 33901	A59	B46	C51	–	E2	E2	–	G29	–	–
KS.KN 47736	A27	B28	C44	D1	E2	E2	F6	G20	H5	I7
KS.KN 47078	A59	B40	C42	D1	E2	E2	F10	G15	H5	I12
KS.KN 47020	A78	B45	C50	D1	E6	E6	F9	G28	H8	I11
KS.KN 47872	A59	B44	C48	D1	E6	E6	F7	G27	H8	I10
KS.KN 47874	A27	B28	C44	D1	E6	E2	F6	G19	H7	I6
KS.KN 47882	A27	B41	C49	D1	E2	E2	F8	G26	H5	I9
KS.KN 47906	A59	B44	C48	–	E1	E1	–	G25	–	–
KS.KN 47907	A27	B43	C47	D1	E6	E6	F6	G24	H8	I8
KS.KN 48312	A73	B41	C45	–	E2	E2	–	G22	–	–
KS.KN 48372	A1	B42	C46	–	E6	E6	–	G23	–	–

In the concatenated *CR* and *Cytb* data (1,631 bp), 119 distinct haplotypes were recognized among 168 individuals (69 newly sequenced). This BI tree exposed two main clades (Figure 2 and Alignment S3), corresponding to the Clades I and II of Lebarbenchon et al. (2010); however, the support values were lower than the previous report. Clade I was in low monophyly with low supported values (0.77 PP and 9% BP), while Clade II had relatively high values (1.0 PP and 50% BP; cf, 1.0/ 93% for Clade I and 0.94 / 76% for Clade II in Lebarbenchon et al., 2010; Figure 2). All samples were divided to Clades I, II, and the others, based on the topology of this BI tree (Figure 2). The others consisted of the individuals of Turkmenistan (C25 and C28), Georgia (C30 and C31), and Ukraine (C32 and C33).

FIGURE 2 A Bayesian phylogenetic tree of concatenated mtDNA *CR* and *Cytb*. Posterior probabilities and maximum-likelihood bootstrap values are shown on nodes. Haplotype names are coincided with Tables 2, S1, and Figure 4. The novel haplotypes are shown with bold. The cluster names are given at the terminal branches. The symbols and colors are corresponding to Figure 3. These cluster-supporting values are shown by bold and italic. The distribution and coalescent time are also indicated. The x marks indicate the individuals from the Black Sea–Caspian Sea region

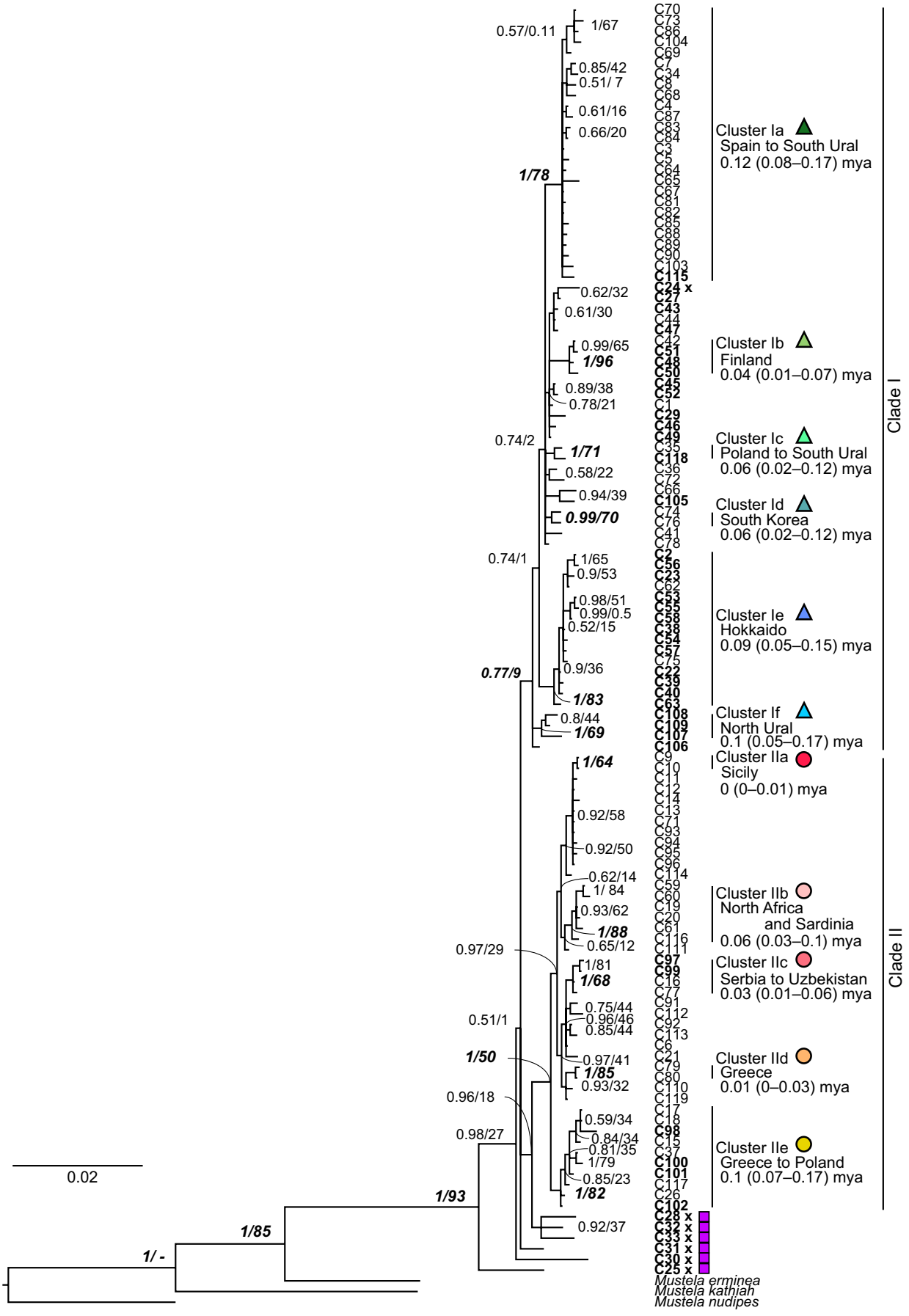
0.57/0.11
1/67
0.85/42
0.51/ 7
0.61/16
0.66/20
1/78
0.62/32
0.61/30
0.99/65
1/96
0.89/38
0.78/21
0.74/2
1/71
0.58/22
0.94/39
0.99/70
0.74/1
1/65
0.9/53
0.98/51
0.99/0.5
0.52/15
0.9/36
0.77/9
1/83
0.8/44
1/69
1/64
0.92/58
0.92/50
0.62/14
1/ 84
0.93/62
1/88
0.65/12
0.97/29
1/81
1/68
0.75/44
0.96/46
0.85/44
0.51/1
1/50
0.97/41
1/85
0.93/32
0.96/18
0.98/27
0.59/34
0.84/34
0.81/35
1/79
0.85/23
1/82
1/93
0.92/37
1/85
1/ -
0.02
C70 C73 C86 C104 C69 C7 C34 C8 C68 C4 C87 C83 C84 C3 C5 C64 C65 C67 C81 C82 C85 C88 C89 C90 C103 C115
Cluster Ia
Spain to South Ural
0.12 (0.08–0.17) mya
C24 x C27 C43 C44 C47 C42 C51 C48 C50 C45 C52 C1 C29 C46 C49 C35 C118 C36 C72 C66 C105 C74 C76 C41 C78
Cluster Ib
Finland
0.04 (0.01–0.07) mya
Cluster Ic
Poland to South Ural
0.06 (0.02–0.12) mya
Cluster Id
South Korea
0.06 (0.02–0.12) mya
C2 C56 C23 C62 C53 C55 C58 C38 C54 C57 C75 C22 C39 C40 C63 C108 C109 C107 C106
Cluster Ie
Hokkaido
0.09 (0.05–0.15) mya
Cluster If
North Ural
0.1 (0.05–0.17) mya
Clade I
C9 C10 C11 C12 C14 C13 C71 C93 C94 C95 C96 C114 C59 C60 C19 C20 C61 C116 C111 C97 C99 C16 C77 C91 C112 C92 C113 C6 C21 C79 C80 C110 C119 C17 C18 C98 C15 C37 C100 C101 C117 C26 C102
Cluster IIa
Sicily
0 (0–0.01) mya
Cluster IIb
North Africa
and Sardinia
0.06 (0.03–0.1) mya
Cluster IIc
Serbia to Uzbekistan
0.03 (0.01–0.06) mya
Cluster IId
Greece
0.01 (0–0.03) mya
Cluster IIe
Greece to Poland
0.1 (0.07–0.17) mya
Clade II
C28 x C32 x C33 x C31 x C30 x C25 x
Mustela erminea
Mustela kathiah
Mustela nudipes

These individuals were located at the most basal position. The ML tree in turn was multifurcated and did not have the main clades (Figure S3).

The *CR* and *Cytb* concatenated BI tree also exhibited eight clusters with high support values (Figure 2). Cluster Ia consisted of individuals from Spain to South Ural. Cluster Ib was shared by individuals from Finland. Cluster Ic distributed in Poland and South Ural. Cluster Ie consisted by only the Hokkaido population. Cluster If included only the North Ural individuals. Cluster IIb was shared by North African individuals and Sardinia. Cluster IId consisted of individuals from Greece, only. Cluster IIe was found from Greece to Poland. In addition, there were three clusters with relatively high support values: Cluster Id was consisted of South Korea, Cluster IIa was shared by Italian and its insular individuals, and Cluster IIc was distributed in Serbia, Bulgaria, and Uzbekistan. Individuals of Honshu Island of Japan shared haplotype C66, which is more closely related to that C105 of a North Ural individual than the Hokkaido population. The locations of clades and clusters were plotted on a Palearctic map (Figure 3).

The mtDNA haplotype network indicated two main clades clearly, compared to the BI tree (Figure 4 and Alignment S4). Clade I was too complicated to read the phylogeographical relationships between haplotypes with many loops indicating the homoplasies. In contrast, Clade II had relatively clear internal structure and the mentioned clusters were supported. Haplotype C28 from Turkmenistan and the Ukrainian C32 and C33 were not placed in either of the two main clades but occupied an intermediate position of them.

3.3 | Diversity in the paternal and biparental genes

Only two *ZFY* haplotypes, D1 and D2, were found from among 30 individuals, of which 29 were newly sequenced in this study. These two haplotypes were strongly diverged, with eight nucleotide differences and an 8-bp indel between them (Figure 5 and Alignment S5). D1 was shared by 12 individuals of Japan (Hokkaido and Honshu), two of Russia and nine of Finland, whereas D2 was common to all six individuals of Bulgaria. The Bulgarian D2 featured the 8-bp insertion, which was also present in the *ZFY* sequence of the closely related *Mustela erminea* (the stoat).

For *ASIP*, 12 haplotypes were detected from 67 individuals obtained in the present study (Figure 5 and Alignment S6), which had 12 polymorphic sites. A central haplotype E1 was found in all regions

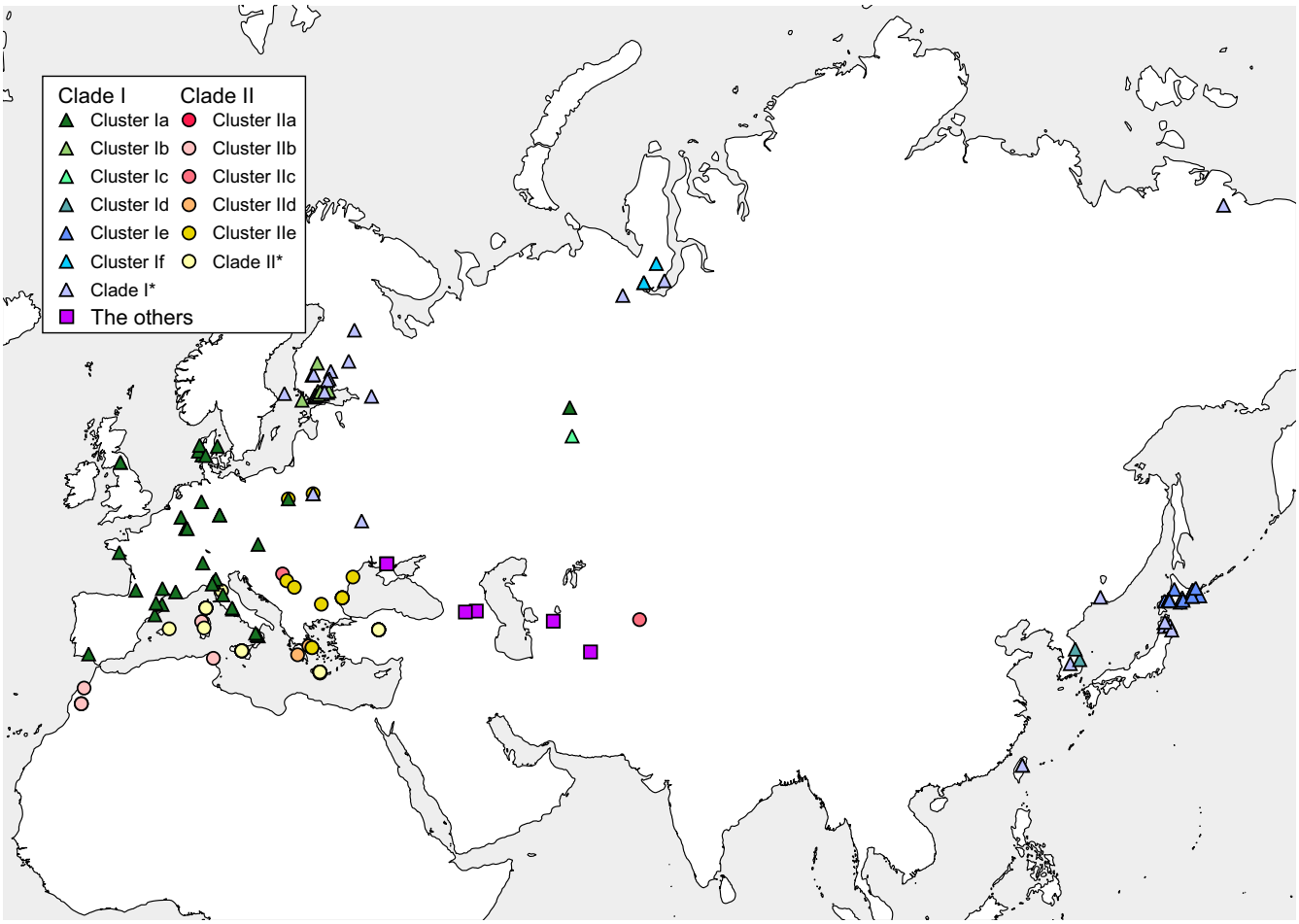

FIGURE 3 Locations of clades and clusters in the Palearctic region. The clade and cluster locations are shown by symbols and colors. Information on localities is the same as Figure 1. The asterisks mean the haplotypes were not grouped to any clusters but included to each clade. The purple means the other haplotypes, which were not included in any clades in Figure 2

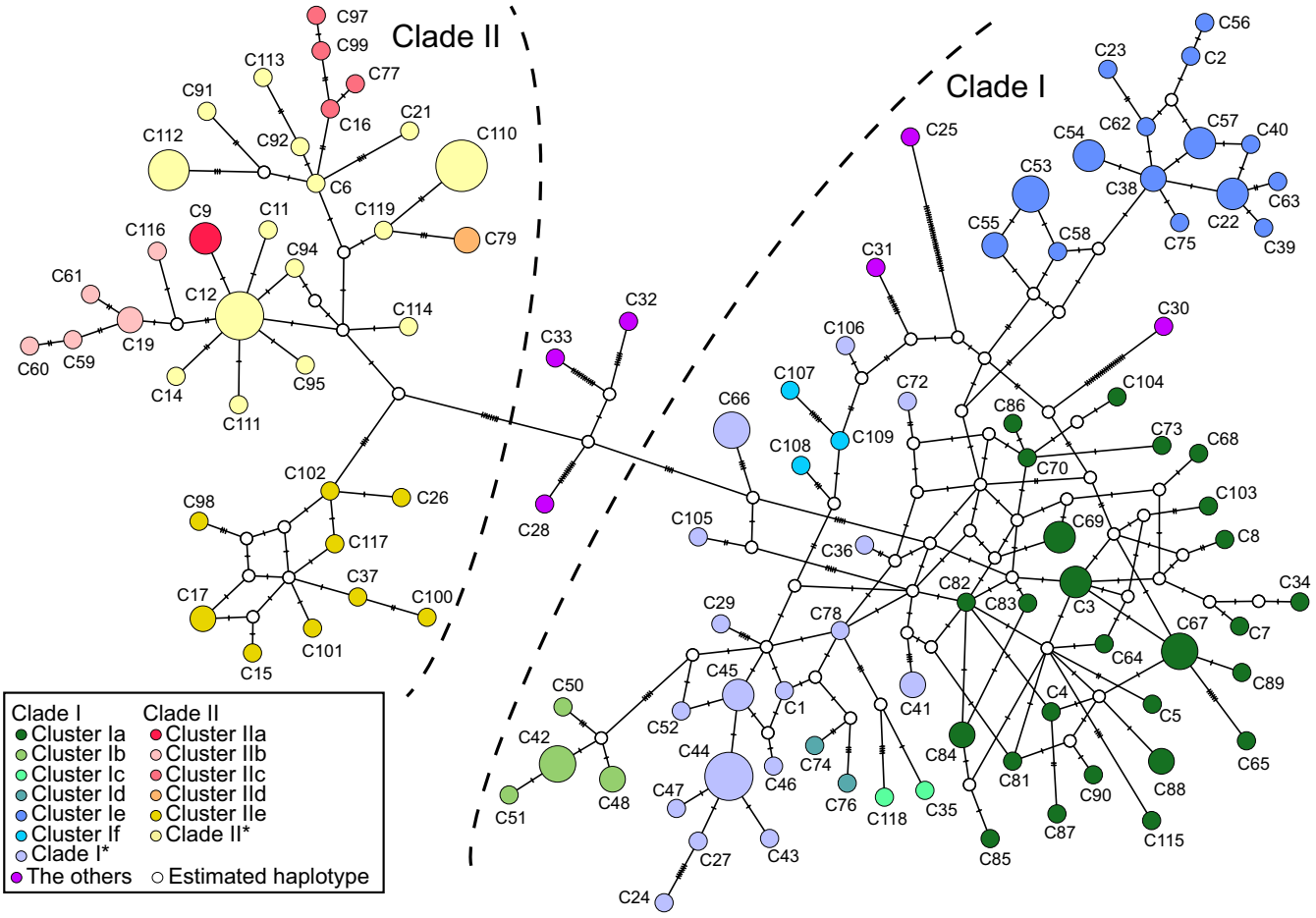

FIGURE 4 A haplotype network of concatenated mtDNA *CR* and *Cytb*. The sizes of circles indicate the proportion of haplotype frequencies. Open circles are estimated haplotypes, and a hatch mark between haplotypes means a nucleotide substitution. Haplotype names are the same as in Figure 2 and Tables 2, S1. The colors are coincided with Figure 3. All samples were divided into each clade or the others, based on Figure 2. The asterisks mean the haplotypes were not grouped to any clusters but included to each clade. The purple circles mean the other haplotypes, which were not included in any clades in Figure 2. If nucleotide sequences of the haplotypes differ by only indels or unresolved nucleotides, they were treated as the same haplotypes in the POPART analysis: C9 and C10; C12, C13, C71, C93 and C96; C17 and C18; C19 and C20; C45 and C49; and C79 and C80

except Honshu, where all individuals shared another haplotype E5. Hokkaido in turn had five haplotypes. However, no further phylogeographical structure was seen, and the differences between haplotypes were just one or two substitutions.

3.4 | Phylogenetic trees from multilocus data

All sequence data on the four loci (mtDNA *CR*, mtDNA *Cytb*, *ZFY*, and *ASIP*) obtained in the present study were concatenated to reconstruct a BI tree (Figure S4a and Alignment S7). This tree consisted of 29 individuals of 2,823 bp with the stoat (*Mustela erminea*) as an outgroup, and the two main clades were supported with higher bootstrap values compared to the mtDNA tree: 92% for Clade I and 98% for Clade II. On the other hands, if *ZFY* was excluded from the data set, no strongly supported major clustering was seen, except for some regional clusters such as Finland, Hokkaido, and Bulgaria (Figure S4 and Alignments S7–S10).

3.5 | Divergence time and population expansion history

The Bayesian phylogram with BEAST analyses, based on the two concatenated mtDNA loci, had a topology similar to that from MrBayes (Figure S5). The time of most recent common ancestor (tMRCA) of the least weasels would have been on 740 (560–940, 95%HPD) thousand years before present (kyBP), at the split of the Turkmenistan lineage (C25) from the others. The coalescence of the remaining lineages would have been 480 (370–600) kyBP. The divergence time of the two main clades could not be traced from this tree, caused by the low PP support (<0.95). The tMRCA of Clade II was 200 (140–270) kyBP. The divergence times of the clusters were also obtained (Figure 2). Based on the demographic fluctuation analysis, both Clades I and II had experienced the population expansion from small populations. Clade II was relatively stable, whereas the expansion of Clade I was more rapid. (Figure 6, and Alignments S11 and S12).

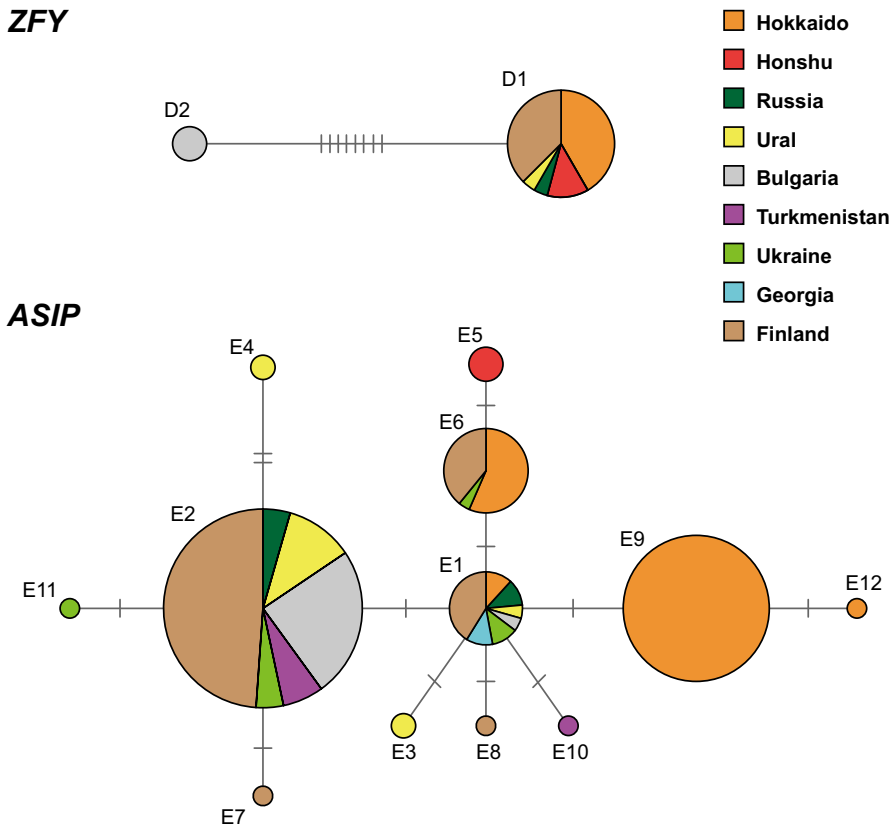

FIGURE 5 Haplotype networks of *ZFY* (a) and *ASIP* (b). The sizes of circles indicate the proportion of haplotype frequencies. Open circles are estimated haplotypes, and a hatch mark between haplotypes means a nucleotide substitution. The haplotype names are the same as Table 2. Individuals from each region are distinguished by using different colors: Hokkaido, orange; Honshu, red; Russia, green; Ural, yellow; Bulgaria, gray; Turkmenistan, purple; Ukraine, light green; Georgia, sky blue; and Finland, light brown

3.6 | Genetic structure

A hierarchical partition of genetic diversity in the concatenated mtDNA *CR* and *Cytb* data by region, and by clade and intra-clade clusters, is shown in Table 3. Overall, the nucleotide diversities were low (shallow genealogy) but haplotype diversities were high. Populations of the Black Sea–Caspian Sea region had the highest nucleotide diversities (0.028 for Turkmenistan; 0.025 for Ukraine; and 0.026 for Georgia), and that of the Ural population (0.009) was also relatively high. Cluster If had the highest nucleotide diversity among clusters. The Honshu population in turn was monomorphic at all loci. Significant values of Tajima's *D* and Fu's F_s statistics are suggestive of the rapid expansion in the Palearctic population. Likewise, treating the mitochondrial lineages separately, Clade I and Cluster Ia show signatures of rapid expansion. The Hokkaido population, Clade II and Cluster IIe, also had significant values of

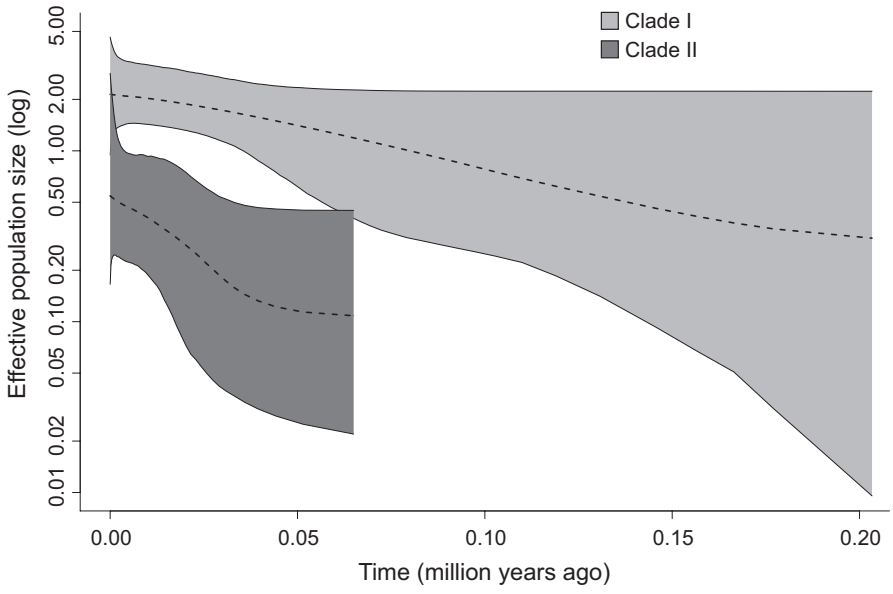

FIGURE 6 Extended Bayesian skyline plots using concatenated mtDNA *CR* and *Cytb* of the least weasels (Clades I and II). Two lines show the range of 95% central posterior density (CPD), and the broken line indicates the median. Plots indicate the population expansion

TABLE 3 Statistical data of the least weasel in Palearctic

Gene	Group	*n*	*h*	*Hd*	π	*D*	F_s
mtDNA	All	168	119	0.992	0.0123	−1.598*	−23.780*
	Hokkaido (Cluster Ie)	26	15	0.948	0.0023	−0.898	−6.035*
	Honshu	4	1	0.000	0.0000	0.000	NA
	Russia†	3	3	1.000	0.0053	0.000	0.987
	Ural	7	7	1.000	0.0090	−1.057	−0.923
	Bulgaria	6	6	1.000	0.0062	0.592	−0.947
	Turkmenistan	2	2	1.000	0.0283	0.000	3.829
	Ukraine	3	3	1.000	0.0251	0.000	2.591
	Georgia	2	2	1.000	0.0258	0.000	3.738
	Finland	22	11	0.875	0.0035	0.591	−0.831
	Clade I	106	71	0.988	0.0084	−1.590*	−24.152*
	Cluster Ia	35	26	0.977	0.0030	−1.614*	−18.823*
	Cluster Ib	8	4	0.750	0.0012	−0.705	0.119
	Cluster Ic	2	2	1.000	0.0037	0.000	1.792
	Cluster Id	2	2	1.000	0.0037	0.000	1.792
	Cluster If	3	3	1.000	0.0053	0.000	0.987
	Clade II	56	41	0.973	0.0059	−1.185	−19.949*
	Cluster IIa	3	2	0.667	0.0000	0.000	NA
	Cluster IIb	6	6	1.000	0.0023	−0.978	−0.905
	Cluster IIc	4	4	1.000	0.0017	0.650	−1.322
	Cluster IId	2	2	1.000	0.0006	0.000	0.000
	Cluster IIe	10	9	0.978	0.0031	−0.301	−3.619*
ASIP	All	67	12	0.780	0.003	−0.702	−3.367
	Hokkaido	25	4	0.478	0.002	0.591	0.479
	Honshu	3	1	0.000	0.0000	0.000	NA
	Russia†	2	2	0.667	0.0014	1.633	0.540
	Ural	5	4	0.733	0.0032	0.324	0.017
	Bulgaria	6	2	0.167	0.0003	−1.141	−0.476
	Turkmenistan	2	2	0.500	0.0021	−0.710	1.099
	Ukraine	3	4	0.867	0.0026	−0.185	−1.350
	Georgia	1	1	1.000	0.0000	0.000	NA
	Finland	20	5	0.631	0.0020	0.047	−0.443
ZFY	All	30	2	0.331	0.0077	0.946	13.074

Note: Asterisks show that values of *D* or F_s are statistically significant ($p < .05$). A dagger means excluded the Ural individuals.
Abbreviations: *D*, Tajima's *D*; F_s, Fu's F_s; *h*, number of haplotypes; *Hd*, haplotype diversity; *n*, number of individuals; NA, not analysis; π, nucleotide diversity.

Fu's F_s. The autosomal *ASIP* showed an overall low nucleotide diversity (0.003) and a high haplotype diversity (0.78). The Y-chromosomal *ZFY* showed relatively low nucleotide and haplotype diversities (0.008 and 0.331). The data of *ZFY* and *ASIP* did not indicate an expansion.

Least weasels had genetic differences to each other (Φ_{st} = 0.556) in the Palearctic, but an attempt to divide the regional populations to subgroups by SAMOVA was not very successful with Alignment S4. A search for the number of independent groups (*K*) that show the maximum inter-group diversity F_{CT} showed that this statistic increased with *K* and did not reach a plateau over *K* = 10 (Figure S6). A configuration of *K* = 3, for which F_{CT} (0.368) was the highest among the others without single-population groups, was very similar to the mtDNA haplotype network (Figure 3). Group I represented populations distributed across the continent from Spain to Japan, which carry the mtDNA Clade I except for Georgia. Group II in turn included populations of Romania, Serbia, Bulgaria, Greece, Turkey, Tunisia, and Morocco, which harbor mtDNA Clade II. Group III was composed of the populations from Turkmenistan and Ukraine (Table 4).

TABLE 4 Population grouping of the least weasels in Palearctic by SAMOVA

	K								
	2	3	4	5	6	7	8	9	10
Hokkaido	I	I	I	I	I	I	I	I	I
Honshu	I	I	II	II	II	II	II	II	II
Russia	I	I	I	II	II	III	III	III	III
Bulgaria	II	II	III	III	III	IV	IV	IV	IV
Turkmenistan	I	III	IV	IV	IV	V	V	V	V
Ukraine	I	III	I	IV	IV	V	V	V	V
Georgia	I	I	I	II	II	III	V	V	VI
Finland	I	I	I	II	II	III	III	III	III
France	I	I	I	V	V	VI	VI	VI	VII
Italy	I	I	I	V	V	VI	VI	VI	VII
Austria	I	I	I	V	VI	VII	VII	VII	VIII
Morocco	II	II	III	III	III	IV	VIII	VIII	IX
Switzerland	I	I	I	V	VI	VII	VII	VII	VIII
Romania	II	II	III	III	III	IV	IV	IV	IV
Greece	II	II	III	III	III	IV	VIII	IX	X
United Kingdom	I	I	I	V	VI	VII	VII	VII	VIII
Poland	I	I	I	V	V	VI	VI	VI	VII
Spain	I	I	I	V	V	VI	VI	VI	VII
Belgium	I	I	I	V	VI	VII	VII	VII	VIII
Germany	I	I	I	V	VI	VII	VII	VII	VIII
Serbia	II	II	III	III	III	IV	IV	IV	IV
Denmark	I	I	I	V	VI	VII	VII	VII	VIII
Luxembourg	I	I	I	V	VI	VII	VII	VII	VIII
South Korea	I	I	I	II	II	III	III	III	III
Uzbekistan	I	I	I	III	II	IV	V	V	III
Taiwan	I	I	I	II	II	III	III	III	III
Tunisia	II	II	III	III	III	IV	VIII	VIII	IX
Turkey	II	II	III	III	III	IV	VIII	IX	X
F_{CT}	0.3410	0.3685	0.3563	0.4010	0.4282	0.4722	0.4702	0.4849	0.5092
F_{ST}	0.6510	0.6507	0.6461	0.5890	0.5820	0.5821	0.5762	0.5751	0.5764
F_{SC}	0.4704	0.4470	0.4502	0.3138	0.2690	0.2083	0.2002	0.1750	0.1368

Note: K is the number of groups.

4 | DISCUSSION

4.1 | Phylogeography of the least weasel in Palearctic

Our data from the concatenated mtDNA *CR* and *Cytb* sequences from a geographically expanded data set demonstrate a confused phylogeographic structure of the least weasels in Palearctic. The tree topologies agree with the two main lineages (Clades I and II) of Lebarbenchon et al. (2010), whereas the support values could not provide full confidence on Clade I's monophyly (Figure 2). Clade I has a broad distribution across northern Palearctic, from Spain in the west to Japan in the east, while Clade II is limited to the South western part of the Palearctic, between North Africa and East Europe. At a lower level, the least weasels were tentatively classified into eleven mtDNA clusters. The Turkmenistan lineage of Central Asia plausibly represents the most ancestral split among all Palearctic populations, as in the data of Kurose et al. (2005).

Our data expanded the coverage of European sampling, for example, Bulgaria and the Urals, supplementing the data of Lebarbenchon et al. (2010) and Rodrigues et al. (2016, 2017). The Bulgarian population was separated into two Clusters (IIc and IIe), and the Northern Urals population consisted of one distinctive Cluster (If) by itself. Individuals from around the Black and Caspian Seas had the new *Cytb* haplotypes that seemed to represent the most ancestral lineages branches of the genealogy (Figure 2).

Furthermore, the Turkmenistan and Ukraine haplotypes appeared at an intermediate position between Clades I and II in the mtDNA haplotype network (Figure 4). This configuration probably brings about the lower confidence values of the main clades, relative to those reported by Lebarbenchon et al. (2010) and McDevitt et al. (2012).

The SAMOVA analysis also suggests the ambiguity for the phylogeographic structure, although the interpopulation component of variation is large (Φ_{st} = 0.556). The data point to a history of demographic and geographic expansions that have taken place across large areas while more ancestral diversity has been retained in certain segments of the range. The nucleotide diversity through the Palearctic population is quite low (0.012), while the haplotype diversity is very high (0.992; Table 3). This suggests that the least weasels experienced a rapid demographic expansion from a small population, as also indicated by the Bayesian simulation, Tajima's *D* and Fu's F_s statistics (Figure 6 and Table 3). Remarkably, similar results were also reported in the closely related species stoat *M. erminea* (Dawson et al., 2014). The data showed low genetic differences and suggested a rapid expansion of *M. erminea* from Spain across the continent and through Beringia to North America. Such continent-wide expansions have also been inferred from other carnivorans, such as Red fox (*Vulpes vulpes* Linnaeus, 1758) and Brown bear (*Ursus arctos* Linnaeus, 1758; Korsten et al., 2009; Statham et al., 2014).

The phylogeographic structure also shows some phenotypic correlates. It seems that Clade II has survived and maintained a relatively constant population size and high genetic diversity in the temperate region in the south western part of the Palearctic, whereas the expansive Clade I represents adaptation to the cold regions. On the other hand, the SAMOVA grouping (*K* = 2) coincided with the distribution of the two coloration types recognized by Abramov and Baryshnikov (2000). Group I correlates with the *nivalis*-type coat color and Group II with the *vulgaris* type. Atmeh, Andruszkiewicz, and Zub (2018) demonstrated a clear relationship between the predation pressure and the camouflage of pelage coloration in a field experiment. One could speculate that this also affected the demographic and evolutionary histories. Clade I (Group I) expanded rapidly across Palearctic including the cold regions.

Our study also for the first time addressed the signals of population history in variation of a biparentally inherited gene *ASIP* and the paternally inherited *ZFY*. The *ASIP* haplotype network, however, did not have any phylogeographic variation (Figure 5). Even the Turkmenistan individual, which had a distinct mtDNA lineage, shared haplotype E2 widespread across the range, in Bulgaria, Urals, Russia, Finland, and Hokkaido. The *ZFY* haplotype network in turn had a distinct subdivision of two main lineages that corresponded with the mtDNA Clade I-II split (Figure 5). Haplotype D1 was distributed from Finland to Japan. This distribution pattern is indeed similar to that in the gray red-backed vole (*Craseomys rufocanus* Sundevall, 1846) which exhibits a monomorphism from western to far eastern Russia, within the partial sequence of the Y-chromosomal DNA (Abramson, Petrova, Dokuchaev, Obolenskaya, & Lissovsky, 2012), and the spatial distribution of mtDNA and Y-chromosomal DNA haplotypes was slightly different. Our spatial distribution of the haplotypes also differed by each gene. As one hypothesis, this discordance could be caused by behavioral differences between sexes of least weasels. The least weasel has the significant sexual dimorphism in body size (greater male vs. female) and sex-biased differences in habitat use (King & Powell, 2007). Furthermore, McDevitt et al. (2013) suggested the dispersal of least weasels was sex-biased toward males. The male wide dispersal could be attributed to the phylogeographical status. In fact, the two main clades are supported with high values if the BI trees included *ZFY* sequences in data sets (Figure S4). Similar conclusions about discordant diversity in multiple loci from the same species have been drawn from other studies, such as Abramson et al. (2012) and Jones and Searle (2015). They also suggested that the discordant may have been caused by the sex biased dispersal in male and female voles and mice. If the male-biased dispersal of least weasels is true, it is easy to suppose that the large males had been strongly affected by cold temperature and could not distribute in high latitude, considering that Zub et al. (2011) suggested larger least weasel had low survival rate in cold environments.

4.2 | Characteristics of clusters and local populations

We recognized some lower-level structure in the mtDNA genealogy of the least weasels, represented by eleven mtDNA clusters with relatively high support values (Figure 2). Three of these Clusters (Ib, Ic, and If) were newly recognized in the present study. Cluster If, only found in the Northern Urals, has the highest intra-cluster diversity. The tMRCA of this cluster was dated approximately 100 kyBP, close to MIS (marine isotope stage) 5c (105–93 kyBP, Räsänen, Huitti, Bhattarai, Harvey, & Huttunen, 2015). The population might then represent a relict that survived the glacial period, and the Ural region would have been one of the cryptic refugia for the species. Actually, based on the paleontological study, Kosintsev, Gasilin, Gimranov, and Bachura (2016) reported the least weasel appeared consistently from MIS 5e in the Ural caves. Likewise, previous studies of other mammalian species also suggested possible refugia in the Ural Mountains. For example, the sables (*Martes zibellina* Linnaeus, 1758; Kinoshita et al., 2015) and the bank voles (*Myodes glareolus* Schreber, 1780; Deffontaine et al., 2005) from the Ural Mountains had relatively higher genetic diversities, suggesting the polymorphic status of relict populations of them. The Ural Mountains were reported as refugia for the common shrews (*Sorex araneus* Linnaeus, 1758) by Polyakov et al. (2001). Cluster Ib consisted of Finnish individuals, and Cluster Ic consisted of just two individuals from Poland and South Ural.

The remaining eight clusters were already reported previously (Kurose et al., 2005, 1999; Lebarbenchon et al., 2010; Rodrigues et al., 2016, 2017). Cluster Ia (=subclade Ia) is now shown to be distributed from Spain to South Urals, and its estimated tMRCA is projected twofold older than by Lebarbenchon et al. (2010) (120 kyBP vs. 62kyBP). Kurose et al. (1999), Kurose et al. (2005) first reported the Cluster Ie

(Hokkaido). This tMRCA was estimated as less than 200 kyBP, but the present study showed around 90 kyBP. The result suggests that ancestors of the Hokkaido population could be prevented to pass the Tsugaru Strait, which separates Honshu and Hokkaido, because that strait was formed around 100–150 kyBP (Ohshima, 1991).

Remarkably, the Honshu population in Japan has no variation on any loci, and this lineage (C66) was more closely related to the North Ural lineage (C106) than the Hokkaido population in the mtDNA analysis. The *ZFY* haplotype D1, however, was shared among Honshu, Hokkaido, and North Ural. The number of chromosomes was also different between the Honshu population ($2n$ = 38) and the Hokkaido population ($2n$ = 42; Obara, 1991). In addition, all studied populations from Eurasia and North America bear the karyotypes similar to that of the Hokkaido population (Mandahl & Fredga, 1980; Zima & Grafodatskij, 1985). According to our result and the previous studies, the migration history could be different between the Honshu and Hokkaido populations.

The Bulgarian individuals were separated into two Clusters (IIc and IIe). Cluster IIc is distributed from Serbia in the Balkan Peninsula to Uzbekistan in Central Asia. Cluster IIe includes the individuals from Greece to Poland and could have experienced the demographic expansion shown by Fu's F_s statistics. Populations around the Black and Caspian Seas (Turkmenistan, Ukraine, and Georgia) had higher nucleotide diversities and were differentiated from the other populations. It has been reported that the populations of the Black and Caspian Seas area could be the ancestor type of least weasel, using morphological characters (Abramov & Baryshnikov, 2000) and mtDNA *CR* (Kurose et al., 2005). Our results emphasize this possibility.

ACKNOWLEDGEMENTS

We would like to thank T. Saitoh, Y. Masuda, H. Yanagawa, F. Sekiyama, M. Takahashi, M. Hisasue, the Finnish Museum of Natural History, and the Museum at the Institute of Plant and Animal Ecology (Ural Branch of the Russian Academy of Sciences) for providing samples, and Y. Nishita for suggestions. This study was supported in part by Joint Research Project Grants from the Japan Society of the Promotion of Science (JSPS) and the Russian Foundation for Basic Research, Russian State program AAAA-A17-117022810195-3, and a grant from the Joint Research Program of the Japan Arctic Research Network Center.

ORCID

Takuma Sato https://orcid.org/0000-0002-0680-6799

Alexei V. Abramov https://orcid.org/0000-0001-9709-4469

Ryuichi Masuda https://orcid.org/0000-0002-6843-0053

REFERENCES

Abramov, A. V., & Baryshnikov, G. F. (2000). Geographic variation and intraspecific taxonomy of weasel *Mustela nivalis* (Carnivora, Mustelidae). *Zoosystematica Rossica*, *8*, 365–402.

Abramson, N. I., Petrova, T. V., Dokuchaev, N. E., Obolenskaya, E. V., & Lissovsky, A. A. (2012). Phylogeography of the gray red-backed vole *Craseomys rufocanus* (Rodentia: Cricetidae) across the distribution range inferred from nonrecombining molecular markers. *Russian Journal of Theriology*, *11*(2), 137–156. https://doi.org/10.15298/rusjtheriol.11.2.04

Atmeh, K., Andruszkiewicz, A., & Zub, K. (2018). Climate change is affecting mortality of weasels due to camouflage mismatch. *Scientific Reports*, *8*(1), 7648. https://doi.org/10.1038/s41598-018-26057-5

Bazinet, A. L., Zwickl, D. J., & Cummings, M. P. (2014). A gateway for phylogenetic analysis powered by grid computing featuring GARLI 2.0. *Systematic Biology*, *63*(5), 812–818. https://doi.org/10.1093/sysbio/syu031

Bergmann, C. (1847). Ueber die Verhaeltnisse der Waermeoekonomie der Thiere zu ihrer Groesse. *Gottinger Studien*, *3*, 595–708.

Bouckaert, R., Heled, J., Kühnert, D., Vaughan, T., Wu, C. H., Xie, D., … Drummond, A. J. (2014). BEAST 2: A software platform for Bayesian evolutionary analysis. *PLoS Computational Biology*, *10*(4), e1003537. https://doi.org/10.1371/journal.pcbi.1003537

Dawson, N. G., Hope, A. G., Talbot, S. L., & Cook, J. A. (2014). A multilocus evaluation of ermine (*Mustela erminea*) across the Holarctic, testing hypotheses of Pleistocene diversification in response to climate change. *Journal of Biogeography*, *41*(3), 464–475. https://doi.org/10.1111/jbi.12221

Deffontaine, V., Libois, R., Kotlík, P., Sommer, R., Nieberding, C., Paradis, E., … Michaux, J. R. (2005). Beyond the Mediterranean peninsulas: Evidence of central European glacial refugia for a temperate forest mammal species, the bank vole (*Clethrionomys glareolus*). *Molecular Ecology*, *14*(6), 1727–1739. https://doi.org/10.1111/j.1365-294X.2005.02506.x

Dellicour, S., & Mardulyn, P. (2014). SPADS 1.0: A toolbox to perform spatial analyses on DNA sequence data sets. *Molecular Ecology Resources*, *14*(3), 647–651. https://doi.org/10.1111/1755-0998.12200

Dupanloup, I., Schneider, S., & Excoffier, L. (2002). A simulated annealing approach to define the genetic structure of populations. *Molecular Ecology*, *11*(12), 2571–2581. https://doi.org/10.1046/j.1365-294X.2002.01650.x

Excoffier, L., & Lischer, H. E. L. (2010). Arlequin suite ver 3.5: A new series of programs to perform population genetics analyses under Linux and Windows. *Molecular Ecology Resources*, *10*(3), 564–567. https://doi.org/10.1111/j.1755-0998.2010.02847.x

Excoffier, L., Smouse, P. E., & Quattro, J. M. (1992). Analysis of molecular variance inferred from metric distances among DNA haplotypes: Application to human mitochondrial DNA restriction data. *Genetics*, *131*(2), 479–491.

Frantz, A. C., McDevitt, A. D., Pope, L. C., Kochan, J., Davison, J., Clements, C. F., … Burke, T. (2014). Revisiting the phylogeography and demography of European badgers (*Meles meles*) based on broad sampling, multiple markers and simulations. *Heredity*, *113*(5), 443–453. https://doi.org/10.1038/hdy.2014.45

Fu, Y. X. (1997). Statistical tests of neutrality of mutations against population growth, hitchhiking and background selection. *Genetics*, *147*(2), 915–925.

Garrick, R. C., Bonatelli, I. A. S., Hyseni, C., Morales, A., Pelletier, T. A., Perez, M. F., … Carstens, B. C. (2015). The evolution of phylogeographic data sets. *Molecular Ecology*, *24*(6), 1164–1171. https://doi.org/10.1111/mec.13108

Hasegawa, M., Kishino, H., & Yano, T. (1985). Dating of the human-ape splitting by a molecular clock of mitochondrial DNA. *Journal of Molecular Evolution*, *22*(2), 160–174. https://doi.org/10.1007/BF02101694

Hewitt, G. (1999). Post-glacial re-colonization of European biota. *Biological Journal of the Linnean Society*, *68*(1–2), 87–112. https://doi.org/10.1111/j.1095-8312.1999.tb01160.x

Hope, A. G., Waltari, E., Dokuchaev, N. E., Abramov, S., Dupal, T., Tsvetkova, A., … Cook, J. A. (2010). High-latitude diversification within Eurasian least shrews and Alaska tiny shrews (*Soricidae*). *Journal of Mammalogy*, *91*(5), 1041–1057. https://doi.org/10.1644/09-MAMM-A-402.1

Hosoda, T., Sato, J. J., Lin, L.-K., Chen, Y.-J., Harada, M., & Suzuki, H. (2011). Phylogenetic history of mustelid fauna in Taiwan inferred from mitochondrial genetic loci. *Canadian Journal of Zoology*, *89*, 559–569. https://doi.org/10.1139/z11-029

Hosoda, T., Suzuki, H., Harada, M., Tsuchiya, K., Han, S.-H.-H., Zhang, Y., … Lin, L.-K.-K. (2000). Evolutionary trends of the mitochondrial lineage differentiation in species of genera *Martes* and *Mustela*. *Genes & Genetic Systems*, *75*(5), 259–267. https://doi.org/10.1266/ggs.75.259

Jones, E. P., & Searle, J. B. (2015). Differing Y chromosome versus mitochondrial DNA ancestry, phylogeography, and introgression in the house mouse. *Biological Journal of the Linnean Society*, *115*(2), 348–361. https://doi.org/10.1111/bij.12522

Kimura, M. (1980). A simple method for estimating evolutionary rates of base substitutions through comparative studies of nucleotide sequences. *Journal of Molecular Evolution*, *16*(2), 111–120. https://doi.org/10.1007/BF01731581

Kimura, M. (1981). Estimation of evolutionary distances between homologous nucleotide sequences. *Proceedings of the National Academy of Sciences of the United States of America*, *78*(1), 454–458. https://doi.org/10.1073/pnas.78.1.454

King, C. M., & Powell, R. A. (2007). *The natural history of weasels and stoats: Ecology, behavior, and management*. Oxford, UK: Oxford University Press.

Kinoshita, G., Sato, J. J., Meschersky, I. G., Pishchulina, S. L., Simakin, L. V., Rozhnov, V. V., … Suzuki, H. (2015). Colonization history of the sable *Martes zibellina* (Mammalia, Carnivora) on the marginal peninsula and islands of northeastern Eurasia. *Journal of Mammalogy*, *96*(1), 172–184. https://doi.org/10.1093/jmammal/gyu021

Korsten, M., Ho, S. Y. W., Davison, J., Pähn, B., Vulla, E., Roht, M., … Saarma, U. (2009). Sudden expansion of a single brown bear maternal lineage across northern continental Eurasia after the last ice age: A general demographic model for mammals? *Molecular Ecology*, *18*(9), 1963–1979. https://doi.org/10.1111/j.1365-294X.2009.04163.x

Kosintsev, P. A., Gasilin, V. V., Gimranov, D. O., & Bachura, O. P. (2016). Carnivores (Mammalia, Carnivora) of the Urals in the Late Pleistocene and Holocene. *Quaternary International*, *420*, 145–155. https://doi.org/10.1016/j.quaint.2015.10.089

*Kurose, N., Abramov, A. V., & Masuda, R. (2000). Intrageneric diversity of the cytochrome *b* gene and phylogeny of Eurasian species of the Genus *Mustela* (Mustelidae, Carnivora). *Zoological Science*, *17*(5), 673–679. https://doi.org/10.2108/zsj.17.673

Kurose, N., Abramov, A. V., & Masuda, R. (2005). Comparative phylogeography between the ermine *Mustela erminea* and the least weasel *M. nivalis* of Palaearctic and Nearctic regions, based on analysis of mitochondrial DNA control region sequences. *Zoological Science*, *22*, 1069–1078. https://doi.org/10.2108/zsj.22.1069

Kurose, N., Masuda, R., & Yoshida, M. C. (1999). Phylogeographic variation in two mustelines, the least Weasel *Mustela nivalis* and the Ermine M. erminea of Japan, based on mitochondrial DNA control region sequences. *Zoological Science*, *16*(6), 971–977. https://doi.org/10.2108/zsj.16.971

Lanave, C., Preparata, G., Saccone, C., & Serio, G. (1984). A new method for calculating evolutionary substitution rates. *Journal of Molecular Evolution*, *20*(1), 86–93. https://doi.org/10.1007/BF02101990

Lanfear, R., Calcott, B., Ho, S. Y. W., & Guindon, S. (2012). Partitionfinder: Combined selection of partitioning schemes and substitution models for phylogenetic analyses. *Molecular Biology and Evolution*, *29*(6), 1695–1701. https://doi.org/10.1093/molbev/mss020

Lebarbenchon, C., Poitevin, F., Arnal, V., & Montgelard, C. (2010). Phylogeography of the weasel (*Mustela nivalis*) in the western-Palaearctic region: Combined effects of glacial events and human movements. *Heredity*, *105*(5), 449–462. https://doi.org/10.1038/hdy.2009.186

Lebarbenchon, C., Poitevin, F., & Montgelard, C. (2006). Genetic variation of the weasel (*Mustela nivalis*) in Corsica based on mitochondrial control region sequences. *Mammalian Biology*, *71*(3), 164–171. https://doi.org/10.1016/j.mambio.2005.11.005

Leigh, J. W., & Bryant, D. (2015). popart: Full-feature software for haplotype network construction. *Methods in Ecology and Evolution*, *6*(9), 1110–1116. https://doi.org/10.1111/2041-210X.12410

Librado, P., & Rozas, J. (2009). DnaSP v5: A software for comprehensive analysis of DNA polymorphism data. *Bioinformatics*, *25*(11), 1451–1452. https://doi.org/10.1093/bioinformatics/btp187

Lorenzen, E. D., Nogues-Bravo, D., Orlando, L., Weinstock, J., Binladen, J., Marske, K. A., … Willerslev, E. (2011). Species-specific responses of Late Quaternary megafauna to climate and humans. *Nature*, *479*(7373), 359–364. https://doi.org/10.1038/nature10574

Magri, D., Vendramin, G. G., Comps, B., Dupanloup, I., Geburek, T., Gömöry, D., … De Beaulieu, J. L. (2006). A new scenario for the Quaternary history of European beech populations: Palaeobotanical evidence and genetic consequences. *New Phytologist*, *171*(1), 199–221. https://doi.org/10.1111/j.1469-8137.2006.01740.x

Mandahl, N., & Fredga, K. (1980). A comparative chromosome study by means of G-, C-, and NOR-bandings of the weasel, the pygmy weasel and the stoat (*Mustela*, Carnivora, Mammalia). *Hereditas*, *93*(1), 75–83. https://doi.org/10.1111/j.1601-5223.1980.tb01045.x

Marciszak, A., & Socha, P. (2014). Stoat *Mustela erminea* Linnaeus, 1758 and weasel *Mustela nivalis* Linnaeus, 1766 in palaeoecological analysis: A case study of Biśnik Cave. *Quaternary International*, *339–340*, 258–265. https://doi.org/10.1016/j.quaint.2013.12.058

McDevitt, A. D., Oliver, M. K., Piertney, S. B., Szafrańska, P. A., Konarzewski, M., & Zub, K. (2013). Individual variation in dispersal associated with phenotype influences fine-scale genetic structure in weasels. *Conservation Genetics*, *14*(2), 499–509. https://doi.org/10.1007/s10592-012-0376-4

McDevitt, A. D., Zub, K., Kawałko, A., Oliver, M. K., Herman, J. S., & Wójcik, J. M. (2012). Climate and refugial origin influence the mitochondrial lineage distribution of weasels (*Mustela nivalis*) in a phylogeographic suture zone. *Biological Journal of the Linnean Society*, *106*(1), 57–69. https://doi.org/10.1111/j.1095-8312.2012.01840.x

McDonald, R. A., Abramov, A. V., Stubbe, M., Herrero, J., Maran, T., Tikhonov, A., … Reid, F. (2016). *Mustela nivalis* (Least Weasel, Weasel). *The IUCN Red List of Threatened Species*, *2016*. https://doi.org/10.2305/IUCN.UK.2016-1.RLTS.T70207409A45200499.en

Mizumachi, K., Nishita, Y., Spassov, N., Raichev, E. G., Peeva, S., Kaneko, Y., & Masuda, R. (2017). Molecular phylogenetic status of the Bulgarian marbled polecat (*Vormela peregusna*, Mustelidae, Carnivora), revealed by Y chromosomal genes and mitochondrial DNA sequences. *Biochemical Systematics and Ecology*, *70*, 99–107. https://doi.org/10.1016/j.bse.2016.10.025

Montgelard, C., Bentz, S., Tirard, C., Verneau, O., & Catzeflis, F. M. (2002). Molecular systematics of sciurognathi (rodentia): The mitochondrial cytochrome b and 12S rRNA genes support the Anomaluroidea (Pedetidae and Anomaluridae). *Molecular Phylogenetics and Evolution*, *22*(2), 220–233. https://doi.org/10.1006/mpev.2001.1056

Obara, Y. (1991). Karyosystematics of the mustelid carnivores of Japan. *Mammalian Science*, *30*(2), 197–220. https://doi.org/10.11238/MAMMALIANSCIENCE.30.197

Ohshima, K. (1991). The late-Quaternary sea-level change of the Japanese Islands. *Journal of Geography (Chigaku Zasshi)*, *100*(6), 967–975. https://doi.org/10.5026/jgeography.100.6_967

Patou, M. L., Chen, J., Cosson, L., Andersen, D. H., Cruaud, C., Couloux, A., … Veron, G. (2009). Low genetic diversity in the masked palm civet *Paguma larvata* (Viverridae). *Journal of Zoology*, *278*(3), 218–230. https://doi.org/10.1111/j.1469-7998.2009.00570.x

Polyakov, A. V., Panov, V. V., Ladygina, T. Y., Bochkarev, M. N., Rodionova, M. I., & Borodin, P. M. (2001). Chromosomal evolution of the common shrew *Sorex araneus* L. from the Southern Urals and Siberia in the Postglacial Period. *Russian Journal of Genetics*, *37*(4), 351–357. https://doi.org/10.1023/A:1016690023394

Räsänen, M. E., Huitti, J. V., Bhattarai, S., Harvey, J., & Huttunen, S. (2015). The SE sector of the Middle Weichselian Eurasian Ice Sheet was much smaller than assumed. *Quaternary Science Reviews*, *122*, 131–141. https://doi.org/10.1016/j.quascirev.2015.05.019

Řičánková, V. P., Robovský, J., Riegert, J., & Zrzavý, J. (2015). Regional patterns of postglacial changes in the Palearctic mammalian diversity indicate retreat to Siberian steppes rather than extinction. *Scientific Reports*, *5*, 12682. https://doi.org/10.1038/srep12682

Rodrigues, M., Bos, A. R., Hoath, R., Schembri, P. J., Lymberakis, P., Cento, M., … Fernandes, C. (2016). Taxonomic status and origin of the Egyptian weasel (*Mustela subpalmata*) inferred from mitochondrial DNA. *Genetica*, *144*(2), 191–202. https://doi.org/10.1007/s10709-016-9889-y

Rodrigues, M., Bos, A. R., Schembri, P. J., de Lima, R. F., Lymberakis, P., Parpal, L., … Fernandes, C. (2017). Origin and introduction history of the least weasel (*Mustela nivalis*) on Mediterranean and Atlantic islands inferred from genetic data. *Biological Invasions*, *19*(1), 399–421. https://doi.org/10.1007/s10530-016-1287-y

Ronquist, F., Teslenko, M., van der Mark, P., Ayres, D. L., Darling, A., Höhna, S., … Huelsenbeck, J. P. (2012). MrBayes 3.2: Efficient Bayesian phylogenetic inference and model choice across a large model space. *Systematic Biology*, *61*(3), 539–542. https://doi.org/10.1093/sysbio/sys029

Sato, J. J., Wolsan, M., Prevosti, F. J., D'Elía, G., Begg, C., Begg, K., … Suzuki, H. (2012). Evolutionary and biogeographic history of weasel-like carnivorans (Musteloidea). *Molecular Phylogenetics and Evolution*, *63*(3), 745–757. https://doi.org/10.1016/j.ympev.2012.02.025

Schmitt, T., & Varga, Z. (2012). Extra-Mediterranean refugia: The rule and not the exception? *Frontiers in Zoology*, *9*(1), 22. https://doi.org/10.1186/1742-9994-9-22

Sheffield, S. R., & King, C. M. (1994). *Mustela nivalis*. *Mammalian Species*, *454*(454), 1–10. https://doi.org/10.2307/3504183

Statham, M. J., Murdoch, J., Janecka, J., Aubry, K. B., Edwards, C. J., Soulsbury, C. D., … Sacks, B. N. (2014). Range-wide multilocus phylogeography of the red fox reveals ancient continental divergence, minimal genomic exchange and distinct demographic histories. *Molecular Ecology*, *23*(19), 4813–4830. https://doi.org/10.1111/mec.12898

Sukumaran, J., & Holder, M. T. (2010). DendroPy: A Python library for phylogenetic computing. *Bioinformatics*, *26*(12), 1569–1571. https://doi.org/10.1093/bioinformatics/btq228

Tajima, F. (1989). Statistical method for testing the neutral mutation hypothesis by DNA polymorphism. *Genetics*, *123*(3), 585–595.

Tamura, K., & Nei, M. (1993). Estimation of the number of nucleotide substitutions in the control region of mitochondrial DNA in humans and chimpanzees. *Molecular Biology and Evolution*, *10*(3), 512–526.

Tamura, K., Stecher, G., Peterson, D., Filipski, A., & Kumar, S. (2013). MEGA6: Molecular Evolutionary Genetics Analysis version 6.0. *Molecular Biology and Evolution*, *30*(12), 2725–2729. https://doi.org/10.1093/molbev/mst197

Tashima, S., Kaneko, Y., Anezaki, T., Baba, M., Yachimori, S., Abramov, A. V., … Masuda, R. (2011). Identification and molecular variations of CAN-SINEs from the ZFY Gene Final Intron of the Eurasian Badgers (Genus *Meles*). *Mammal Study*, *36*(1), 41–48. https://doi.org/10.3106/041.036.0105

Vereshchagin, N. K., & Baryshnikov, G. F. (1992). The ecological structure of the "mammoth fauna" in Eurasia. *Annales Zoologici Fennici*, *28*, 253–259. https://doi.org/10.1016/j.quaint.2004.04.011

Yamada, C., & Masuda, R. (2010). Molecular phylogeny and evolution of sex-chromosomal genes and SINE Sequences in the Family Mustelidae Molecular phylogeny and evolution of sex-chromosomal genes and SINE sequences in the family Mustelidae. *Mammal Study*, *35*(1), 17–30. https://doi.org/10.3106/041.035.0102

Youngman, P. M. (1993). The Pleistocene small carnivores of Eastern Beringia. *The Canadian Field-Naturalist*, *107*(2), 139–163.

Zima, J., & Grafodatskij, A. S. (1985). C-heterochromatic arm variation in the weasel, *Mustela nivalis* (Mustelidae, Carnivora). *Folia Zoologica*, *34*, 125–132.

Zub, K., Szafrańska, P. A., Konarzewski, M., & Speakman, J. R. (2011). Effect of energetic constraints on distribution and winter survival of weasel males. *The Journal of Animal Ecology*, *80*(1), 259–269. https://doi.org/10.1111/j.1365-2656.2010.01762.x

SUPPORTING INFORMATION

Additional supporting information may be found online in the Supporting Information section at end of the article.

Alignment S1. CR for Figure S1.nexus.

Alignment S2. Cytb for Figure S2.nexus.

Alignment S3. CR and Cytb for Figure 2, S3 and S5.nexus.

Alignment S4. CR and Cytb for Figure 4.nexus.

Alignment S5. ZFY for Figure 5a.nex.

Alignment S6. ASIP for Figure 5b.nex.

Alignment S7. CR, Cytb, ASIP and ZFY for Figure S4a.nex.

Alignment S8. CR, Cytb and ASIP for Figure S4b.nex.

Alignment S9. CR, Cytb and ZFY for Figure S4c.nex.

Alignment S10. ZFY and ASIP for Figure S4d.nex.

Alignment S11. Clade I for Figure 6.nex.

Alignment S12. Clade II for Figure 6.nexus.

Figure S1. A Bayesian phylogenetic tree of mtDNA control region (*CR*). The posterior probabilities and maximum likelihood bootstrap values are shown on nodes. The haplotype names are coincided with Table 2 and Table S1.

Figure S2. A Bayesian phylogenetic tree of mtDNA cytochrome *b* (*Cytb*). The posterior probabilities and maximum likelihood bootstrap values are shown on nodes. The haplotype names are coincided with Table 2 and Table S1.

Figure S3. A maximum likelihood phylogenetic tree of concatenated mtDNA *CR* and *Cytb*. The maximum likelihood bootstrap values are shown on nodes. The haplotype names are coincided with Table 2 and Table S1.

Figure S4. The Bayesian phylogenetic tree of each pair: (a) The BI tree of concatenated all loci; (b) The BI tree of concatenated *CR*, *Cytb* and *ASIP*; (c) The BI tree of concatenated *CR*, *Cytb* and *ZFY*; (d) The BI tree of concatenated *ZFY* and *ASIP*. The posterior probabilities and maximum likelihood bootstrap values are shown on nodes. The haplotype names coincided with Table 2 and Table S1.

Figure S5. A Bayesian chronogram of mtDNA. The numbers at nodes are the clade numbers for clades with ≥0.95 posterior probabilities, and the coalescent times are represented in table (inset). Node bars show the 95% highest posterior density of nodal age estimates. The *x* marks indicate the individuals from the Black Sea-Caspian Sea region.

Figure S6. The results of SAMOVA analysis for mtDNA data set. The number of group (*K*) is shown on the *x*-axes. The *F* values were shown on the y-axes. F_{ct}; square, F_{st}; circle, F_{sc}; triangle.

Table S1. References from GenBank.

Table S2. Primers for PCR amplification and sequencing.

Table S3. Nucleotide substitution models for reconstructing phylogenetic trees. C1, C2 and C3 mean the first, second and third codons for *Cytb*.

How to cite this article: Sato T, Abramov AV, Raichev EG, et al. Phylogeography and population history of the least weasel (*Mustela nivalis*) in the Palearctic based on multilocus analysis. *J Zool Syst Evol Res*. 2020;58:408–426. https://doi.org/10.1111/jzs.12330